Part I
Wellbeing and Health Futures

Chapter 1

Plasma Polymerized Nanoparticles: From Cell Imaging to Cancer Therapy

Behnam Akhavan[1,2,3]*, Elmer S. Austria Jr.[1], Deepu Ashok[1], Kevinilo P. Marquez[4], and Jukkrit Nootem[5]

[1]School of Biomedical Engineering, The University of Sydney, Sydney, NSW 2006, Australia
[2]School of Engineering, College of Engineering, Science and Environment, University of Newcastle, Callaghan, NSW 2308, Australia
[3]Hunter Medical Research Institute (HMRI), Precision Medicine Program, New Lambton Heights, NSW 2305, Australia
[4]Institute for Frontier Materials, Deakin University, Geelong, Victoria 3216, Australia
[5]School of Chemistry, The University of Sydney, Sydney, NSW 2006, Australia

Abstract

Cancer remains a leading cause of mortality worldwide, lacking effective targeted therapies. In Australia alone, more than 50,000 people die from cancer each year. Polymeric nanoparticles (NPs) are promising platforms for cancer nanomedicine due to their tuneable physicochemical properties, biocompatibility, and capacity for functionalisation. However, conventional wet-chemical synthesis often relies on toxic solvents, complex purification, and limited scalability, restricting clinical translation. Plasma polymerisation offers a dry, solvent-free, and sustainable alternative for generating polymeric nanoparticles (PPNs) with unique surface chemistries and embedded long-lived radicals that enable direct covalent attachment of biomolecules without chemical linkers. Here, we demonstrate the versatility of PPNs by separately conjugating two fluorescent dyes (Nile Blue A and Rhodamine-1) for imaging, and two cytotoxic agents (Doxorubicin and Curcumin) for therapy. Fluorophore-conjugated PPNs facilitated visualisation of cellular uptake in A549 lung and MDA-MB-231 breast cancer cells, confirming their potential for diagnostic imaging. Therapeutic PPN formulations (PPN-DOX and PPN-Cur) localised around the nucleus and membrane of MDA-MB-231 cells and significantly reduced cell viability, with cytotoxicity corroborated by LDH leakage assays. These findings demonstrate the multifunctionality of PPNs as efficient nanocarriers for combined imaging and therapeutic applications. This streamlined, chemical-free approach overcomes key limitations of polymeric nanomedicine, including the reliance on hazardous solvents, multistep conjugation, and scalability issues. The PPNs prototype represents a paradigm shift in cancer nanomedicine: a universal, sustainable, and adaptable drug delivery platform, transforming precision therapies with global relevance and tangible impact for humanity.

Keywords: *Plasma polymerization, Nanoparticles, Cancer Therapy, Imaging, Drug Delivery*

Introduction

Cancer remains one of the highest causes of mortalities worldwide, ranking second behind ischemic heart disease, with about 8.97 million deaths in 2019[1]. The high mortality is partly driven by the intrinsic heterogeneity of cancer subtypes, which hinders the development of universal treatments. Despite advances in chemotherapy, pharmacotherapy, and radiotherapy, clinical outcomes are often limited by suboptimal efficacy, systemic toxicity, and non-specific biodistribution, leading to damage of healthy tissues[2]. Furthermore, multidrug resistance significantly reduces the effectiveness of these interventions[3].

Free drugs, administered without a drug delivery system, face pharmacokinetic limitations such as rapid clearance, poor stability, and low tumour accumulation[4]. Nanoparticle (NP)-based drug delivery systems address these issues by encapsulating or conjugating drugs within nanoscale carriers[5], improving solubility, prolonging circulation, and enhancing tumour accumulation via the enhanced permeability and retention effect[6]. Among these, NP-based carriers, polymeric NPs, are especially attractive due to their tuneable structure, biocompatibility, and ability to navigate complex biological environments[7]. Their amphiphilic matrices enable colloidal stability, functional surfaces allow ligand conjugation, and stimuli-responsive features permit triggered drug release. However, wet chemical synthesis is often hampered by toxic solvents, multiple purification steps, and poor scalability, limiting clinical translation[8,9].

---

[1]Camilla Mattiuzzi and Giuseppe Lippi, "Current Cancer Epidemiology," *Journal of Epidemiology and Global Health* 9 (2019): 217–22, https://doi.org/10.2991/jegh.k.191008.001

[2]Zihan Wang et al., "Poly Ethylene Glycol (PEG)-Based Hydrogels for Drug Delivery in Cancer Therapy: A Comprehensive Review," *Advanced Healthcare Materials* 12, no. 18 (April 13, 2023): e2300105, https://doi.org/10.1002/adhm.202300105

[3]Hira Choudhury et al., "Rising Horizon in Circumventing Multidrug Resistance in Chemotherapy With Nanotechnology," *Materials Science and Engineering C* 101 (2019): 596–613, https://doi.org/10.1016/j.msec.2019.04.005

[4]Boyu Su et al., "Therapeutic Regulation of Epigenetics in Cancer Treatment Through Drug Delivery Systems," *Nano Today* 56 (2024): 102251, https://doi.org/10.1016/j.nantod.2024.102251

[5]Bijaideep Dutta, K.C. Barick, and P.A. Hassan, "Recent Advances in Active Targeting of Nanomaterials for Anticancer Drug Delivery," *Advances in Colloid and Interface Science* 296 (August 18, 2021): 102509, https://doi.org/10.1016/j.cis.2021.102509

[6]Michael J. Mitchell et al., "Engineering Precision Nanoparticles for Drug Delivery," *Nature Reviews Drug Discovery* 20 (2021): 101–24, https://doi.org/10.1038/s41573-020-0090-8

[7]Karine Cappuccio De Castro, Josiel Martins Costa, and Maria Gabriela Nogueira Campos, "Drug-loaded Polymeric Nanoparticles: A Review," *International Journal of Polymeric Materials* 71, no. 1 (August 7, 2020): 1–13, https://doi.org/10.1080/00914037.2020.1798436

[8]Elmer S. Austria and Behnam Akhavan, "Polymeric Nanoparticle Synthesis for Biomedical Applications: Advancing from Wet Chemistry Methods to Dry Plasma Technologies," *Nanoscale* 17, no. 21 (2025): 13020–56, https://doi.org/10.1039/d5nr00436e

[9]Elmer Austria et al., "Breaking Biological Barriers: Engineering Polymeric Nanoparticles for Cancer Therapy," *Nano Today* 60 (2025): 102552, https://doi.org/10.1016/j.nantod.2024.102552

Plasma polymerisation provides a solvent-free and sustainable method for synthesising polymeric NPs[10]. It proceeds through a fragmentation-recombination pathway, where cold temperature plasma discharges of precursor organic gases or vapours break monomers into reactive species, including electrons, ions, radicals, and molecular fragments. Such highly reactive species undergo recombination and crosslinking, forming highly branched and crosslinked polymeric nano-thin films or NPs[11]. The resulting NPs contain long-lived radicals that act as anchorage sites for covalent biomolecule attachment[12], eliminating the need for chemical linkers or toxic solvents.

Here, we demonstrate the versatility of plasma-polymerized nanoparticles (PPNs) by conjugating two fluorescent dyes (Nile Blue A, Rhodamine-1) and two therapeutic agents (Doxorubicin, Curcumin) for cancer therapy. Fluorophore-conjugated PPNs enabled real-time tracking of cellular uptake, while drug-conjugated PPNs suppressed cancer cell proliferation, highlighting their dual role in imaging and therapy. This streamlined, chemical-free approach addresses key challenges in polymeric nanomedicine, including scalability and environmental sustainability. This technology offers a transformative platform for advancing multifunctional NPs in cancer diagnosis and treatment.

Materials and Methods

PPNs were generated in a stainless-steel vacuum chamber (Figure **1**a) using acetylene, nitrogen, and argon as precursor gases at flow rates of 6, 10, and 3 sccm, respectively. The chamber was maintained at a base pressure of 5×10^{-5} Torr. Plasma discharge was initiated by applying 150 W of radiofrequency (13.56 MHz) power to the top electrode for 390 s, as previously described in our earlier works[13-15]. The resulting PPNs were subsequently collected in a commercial 24-well cell culture plate.

Covalent surface functionalisation of PPNs with Nile Blue A (NB), Rhodamine-1 (Rho1), Doxorubicin (DOX), or Curcumin (Cur) was achieved through a single-step incubation. Each biomolecule was added to PPN suspensions in Milli-Q water at a ratio of 200 pg per 100,000 particles and agitated for 1 h at room temperature. The resulting conjugates were purified by centrifugation (8000 rcf), followed by

[10]Miguel Santos et al., "Plasma Synthesis of Carbon-Based Nanocarriers for Linker-Free Immobilization of Bioactive Cargo," *ACS Applied Nano Materials* 1, no. 2 (January 5, 2018): 580–94, https://doi.org/10.1021/acsanm.7b00086

[11]Masoud Zhianmanesh et al., "Plasma Surface Functionalization: A Comprehensive Review of Advances in the Quest for Bioinstructive Materials and Interfaces," *Applied Physics Reviews* 10, no. 2 (2023): 021301, https://doi.org/10.1063/5.0130829

[12]Laura Libnan Haidar et al., "Direct Covalent Attachment of Fluorescent Molecules on Plasma Polymerized Nanoparticles: A Simplified Approach for Biomedical Applications," *Journal of Materials Chemistry B* 13, no. 5 (2025): 1666–80, https://doi.org/10.1039/d4tb01515k

[13]Behnam Akhavan et al., "Radical-functionalized Plasma Polymers: Stable Biomimetic Interfaces for Bone Implant Applications," *Applied Materials Today* 16 (2019): 456–73, https://doi.org/10.1016/j.apmt.2019.07.002

[14]Laura L. Haidar et al., "Surface-Active Plasma-Polymerized Nanoparticles for Multifunctional Diagnostic, Targeting, and Therapeutic Probes," *ACS Applied Nano Materials* 5, no. 12 (August 30, 2022): 17576–91, https://doi.org/10.1021/acsanm.2c03213

[15]Miguel Santos et al., "Substrate Geometry Modulates Self-assembly and Collection of Plasma Polymerized Nanoparticles," *Communications Physics* 2, no. 52 (May 20, 2019): 1–11, https://doi.org/10.1038/s42005-019-0153-5

resuspension in Milli-Q water. This washing cycle was repeated three times before resuspending the final product in 5 mL of PBS for material characterisation and in-vitro experiments.

Surface chemistry and elemental composition were analysed by X-ray photoelectron spectroscopy (XPS, Thermo Fisher K-Alpha+). Morphological features were examined by scanning electron microscopy (SEM, JEOL JSM 7800F), while hydrodynamic diameters were determined via dynamic light scattering (DLS, Malvern Zetasizer Nano ZS). Functional groups were identified by Fourier-transform infrared spectroscopy (FTIR, Bruker ALPHA with ATR diamond module). Radical content was assessed using electron paramagnetic resonance (EPR, SpinScanX, Adani). Fluorescence spectra of PPN-NB, PPN-Rho1, PPN-DOX, and PPN-Cur were recorded using a ClarioStar Plus plate reader (BMG Labtech) at excitation/emission maxima of 624/680, 560/584, 470/596, and 425/544 nm, respectively.

A549 (lung) and MDA-MB-231 (breast) cancer cells were seeded at 30,000 cells/dish and cultured overnight at 37 °C in a 5% CO_2 incubator. Cells were then incubated with either PPN-NB or PPN-Rho1 (50 μg/mL in Adv-DMEM) for 1 h. After treatment, cells were washed three times with PBS and resuspended in FluoroBrite™ DMEM. Confocal imaging was performed using an Olympus FluoView FV3000 microscope (excitation: 640 nm; emission: 655-735 nm). Image analysis was conducted with Fiji software.

The therapeutic potential of PPN-DOX and PPN-Cur was evaluated in MDA-MB-231 cells using Alamar Blue assay. Cells were seeded at 5000 cells/well in 96-well plates and allowed to adhere for 24 h. Samples containing varying concentrations of PPN-DOX or PPN-Cur were added and incubated for 48 h. Following treatment, 10 μL of resazurin reagent was introduced into each well and incubated for 4 h. Fluorescence was recorded at 570 nm using a ClarioStar plate reader. Cell viability was expressed relative to PBS-treated controls, with 5% SDS serving as a positive control. Data were processed in OriginPro 2022 (OriginLab, USA).

Results and Discussion

Plasma Polymerisation of NPs

PPNs are synthesised using a dry, linker-free and environmentally sustainable technology that harnesses plasma, the fourth state of matter, to initiate polymerisation. The process is conducted in a custom-built stainless-steel reactor operating under low pressure (~10^{-5} Torr), powered by a radiofrequency (RF) generator connected to the top electrode to generate a stable plasma discharge (Figure **1**a). Within this plasma environment, the gaseous precursor mixture undergoes fragmentation into reactive species, which subsequently nucleate and aggregate into protoparticles, ultimately forming PPNs (Figure **1**b).

PPNs benefit from favourable physicochemical properties which is crucial in its role as a nanoplatform for delivering biomolecular payload in the body. The PPNs created from a precursor gas mixture of argon, nitrogen, and acetylene are composed of carbon (64.1 atm%), nitrogen (28.3 atm%), and oxygen (7.6 atm%), as informed by the X-ray photoelectron spectroscopy (XPS) survey spectrum presented in Figure **2**a. Scanning electron microscopy (SEM) imaging reveals that the PPNs have spherical morphology, with dry particle size ranging from 70 to 120 nm (Figure **2**b and Figure **2**c). The low

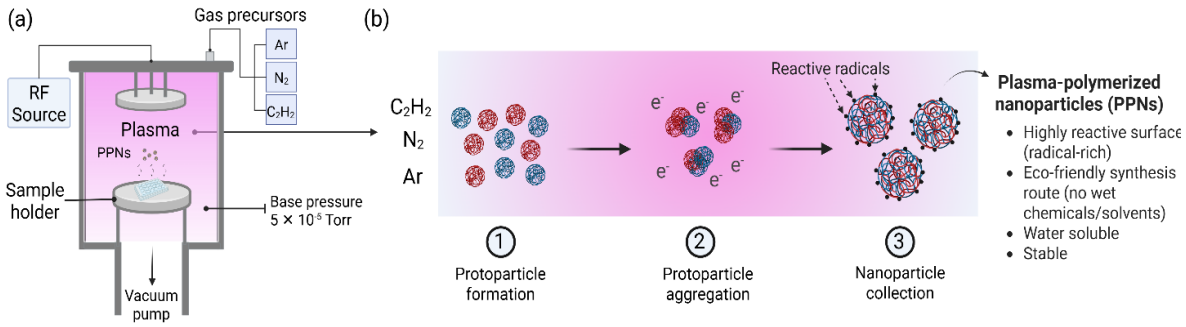

Figure 1: Schematic representation of the production of the PPN prototype. (a) Custom-built cylindrical vacuum chamber used for plasma polymerisation of NPs. (b) Synthesis pathway illustrating the plasma-induced fragmentation of precursor gases (C_2H_2, N_2, and Ar), leading to the nucleation and accretion of protoparticles. Once a critical mass is reached, the PPNs settle into a 24-well collection plate under gravitational force.

polydispersity index (PDI) value (<0.1) in water suggests monodispersity in aqueous solutions (Figure **2**d), along with relatively small hydrodynamic size (D_H = 190 nm) as measured using dynamic light scattering (DLS), which are both important in overcoming biological barriers of delivery. PPNs contain surface functional groups such as hydroxyl, amine, nitrile, and carboxylic acid moieties as seen in the attenuated total reflectance - Fourier transform infrared (ATR-FTIR) spectra (Figure **2**e). The relative abundance and composition of these moieties can be tuned by altering precursor gas composition, enabling tailored surface chemistries for specific applications such as covalent drug conjugation, targeted ligand attachment, or modulation of cellular interactions. The defining feature of PPNs is the presence of unpaired electrons or radicals in its nanostructure, detected through electron paramagnetic resonance (EPR) spectroscopy (Figure **2**f), which gradually diffuse towards the material's surface. These radicals enable robust and chemical-free covalent attachment of virtually any biomolecule onto the PPN surface.

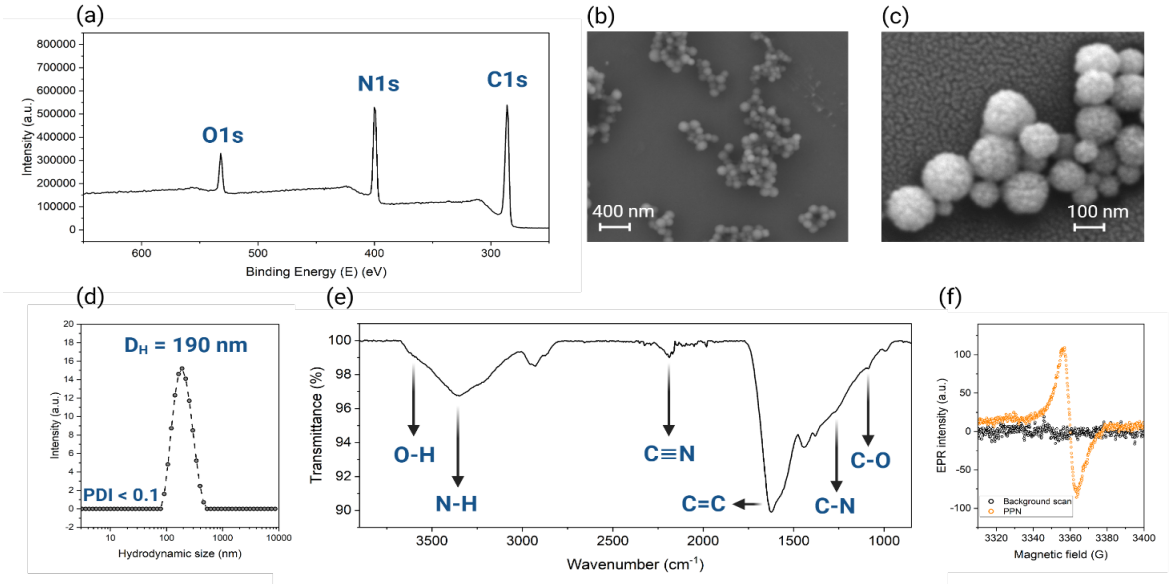

Figure 2: Physicochemical properties of PPNs enable it to become ideal nanoplatforms of transporting biomolecules. (a) X-ray photoelectron spectroscopy survey spectra of PPNs, (b-c) SEM micrographs, (d) dynamic light scattering spectra, (e) Fourier transform infrared spectra, and (f) electron paramagnetic resonance spectra of PPNs.

Covalent Attachment of Biomolecular Payload onto PPN Surfaces

To demonstrate the robustness and versatility of the PPN platform, four representative molecules (NB, Rho1, DOX, and Cur) were covalently conjugated in a single-step process under mild conditions without chemical linkers and toxic solvent. NB and Rho1 are fluorescent dyes commonly used in cellular imaging[16,17], while DOX and Cur are cytotoxic agents previously explored in cancer therapy[18-19]. Both PPNs and each respective payloads were dispersed in water (or ethanol for Cur) and were incubated for 1 h at room temperature (Figure **3**a).

Following SDS washing, all four PPN formulations (PPN-NB, PPN-Rho1, PPN-DOX, and PPN-Cur) exhibited statistically significant increases in fluorescence intensity ($P < 0.0001$) compared to their unconjugated counterparts (Figure **4**a). The retention of strong fluorescence after stringent washing confirms stable covalent bonding between the payloads and the PPN surfaces.

Beyond the observed fluorescence signals, further evidence of successful conjugation was obtained from the high-resolution XPS C1s spectra. Each molecule exhibited distinct surface functional groups, and these variations were consistently reflected in their corresponding C1s spectral peaks. The C1s spectrum of unconjugated PPN shows three characteristic components at binding energies (BE) of 284.9 eV (C–C/C–H), 286.4 eV (C–N/C–O), and 288.1 eV (C=O). Upon conjugation with NB, appeared at ~283.3 eV, corresponding to sp^2-hybridised C=C from the phenoxazine moiety in Nile Blue A. In the case of Rho1, the relative abundance of the C-N species increased from 19.1% for the unconjugated PPN to 42.4% for the PPN-Rho1 due to the presence of amino groups on the central xanthene ring in Rho1. The shape of the high-resolution C1s peaks of PPN-DOX and PPN-Cur both display a defined shoulder peak at 286.4 eV which corresponds to an increase in C-N/C-O species. For DOX, this increase from 19.1% pre-conjugation to 30.9% after attachment came from the daunosamine sugar moiety. The ketone group in DOX also resulted to a 2.4% increase in C=O species. In contrast, the prominent shoulder peak in PPN-Cur is caused by increase in C-O species coming from the *o*-methoxy and phenolic groups in Cur. These two functional groups almost doubled the relative abundance of C-N/C-O species from 19.1% to 38.0% in PPN-Cur. Taken together, these data provide compelling evidence for the successful covalent attachment of all four biomolecules (NB, Rho1, DOX, and Cur) onto the nanoparticle surface, firmly validating the robustness and versatility of the PPN prototype.

---

[16]Haidar et al., "Direct Covalent Attachment of Fluorescent Molecules on Plasma Polymerized Nanoparticles: A Simplified Approach for Biomedical Applications."

[17]Nian Kee Tan et al., "Ultrasensitive Dual Fluorophore-Conjugated Carbon Dots for Intracellular pH Sensing in 3D Tumor Models," *ACS Applied Materials & Interfaces* 16, no. 36 (August 31, 2024): 47303–13, https://doi.org/10.1021/acsami.4c10836

[18]Oktay Tacar, Pornsak Sriamornsak, and Crispin R Dass, "Doxorubicin: An Update on Anticancer Molecular Action, Toxicity and Novel Drug Delivery Systems," *Journal of Pharmacy and Pharmacology* 65, no. 2 (2013): 157–70, https://doi.org/10.1111/j.2042-7158.2012.01567.x

[19]Shiva Shakori Poshteh, Shohreh Alipour, and Pegah Varamini, "Harnessing Curcumin and Nanotechnology for Enhanced Treatment of Breast Cancer Bone Metastasis," *Discover Nano* 19, no. 177 (November 11, 2024), https://doi.org/10.1186/s11671-024-04126-1

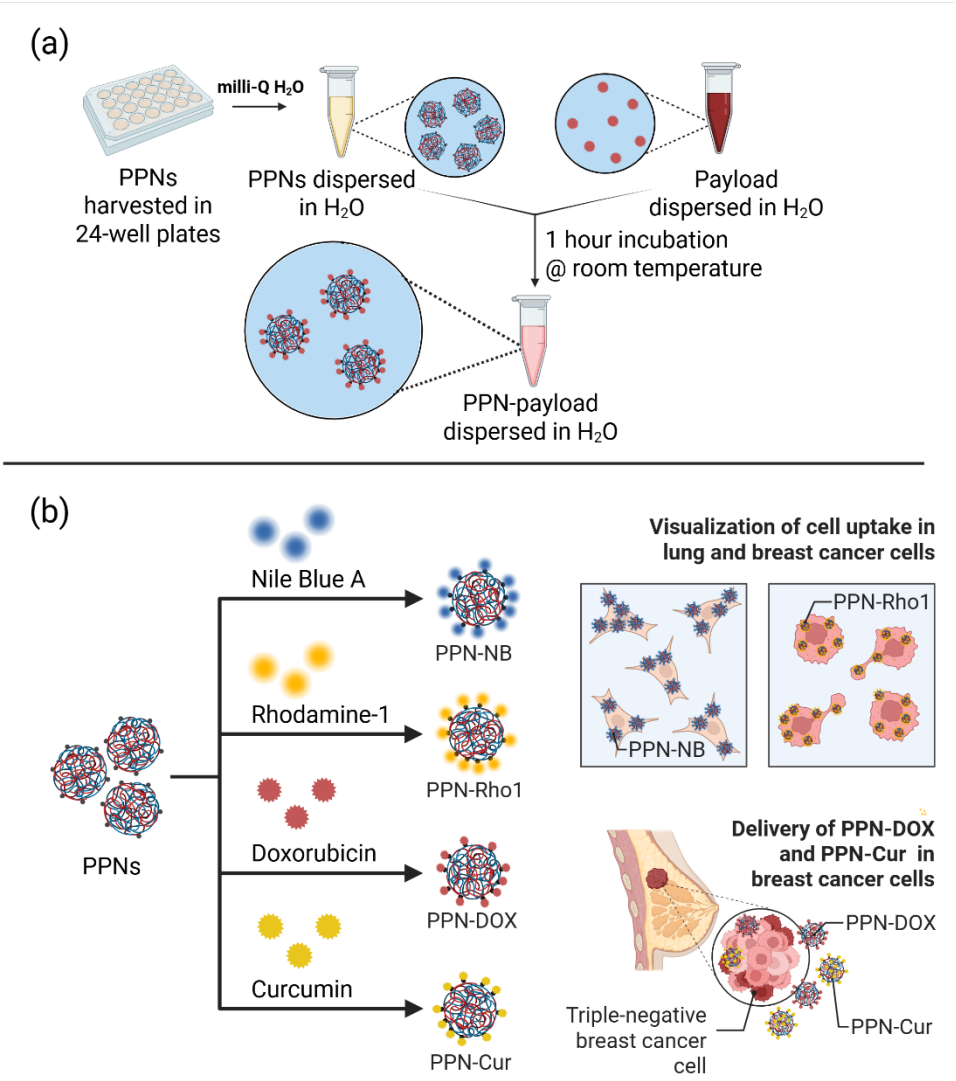

Figure 3: (a) Single-step, covalent conjugation of PPNs with payload. (b) PPNs were conjugated with fluorophore dyes (NB, Rho1) and cytotoxic agents (DOX, Cur) and were used for cell imaging and cancer therapy.

Cellular Uptake and Cytotoxicity Studies on PPNs

Nanoplatforms such as PPNs can serve as carriers for delivering imaging agents to cells and tissues, with excellent potential in diagnostic imaging applications. The performance of fluorophore-labelled PPNs was evaluated by examining their cellular uptake across different cancer cell lines. The fluorescently tagged nanocarriers enabled direct visualisation of nanoparticle internalisation. Specifically, PPN-NB was incubated with A549 lung carcinoma cells, while PPN-Rho1 was introduced to MDA-MB-231 triple-negative breast cancer cells (Figure **3**b).

As shown in the confocal laser scanning microscopy images presented in Figure **5**a, A549 cells effectively internalized the PPN-NB formulation. After a 1-hour incubation, intracellular localisation was verified through the detection of blue fluorescence corresponding to the NB dye. In contrast, no fluorescence was observed in cells exposed solely to unconjugated PPN cores, validating that the detected emission originated exclusively from the conjugated NB fluorophore.

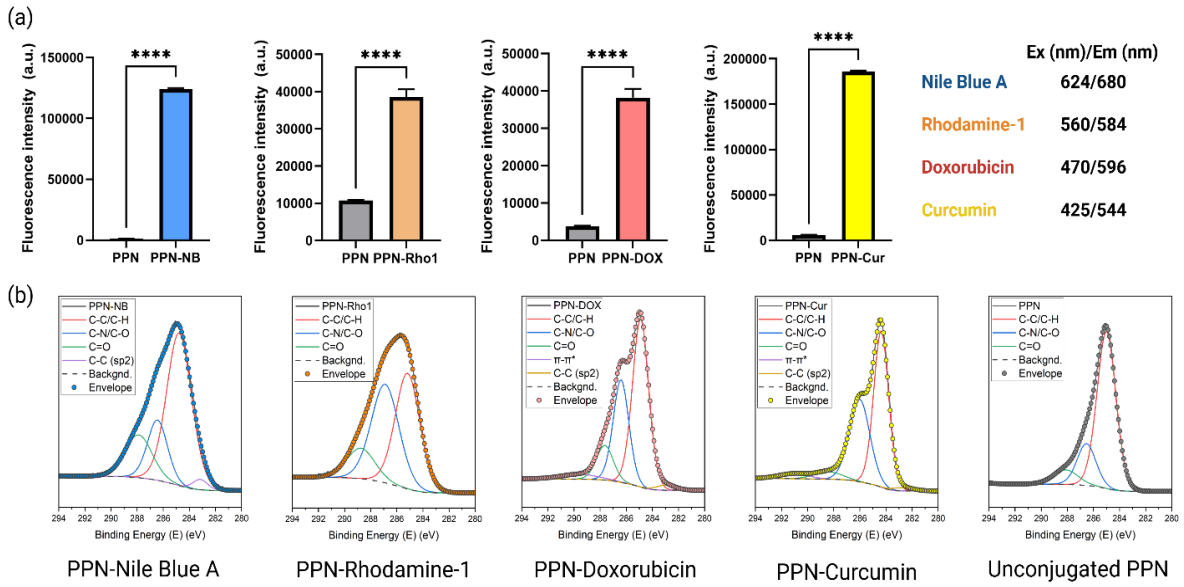

Figure 4: Covalent conjugation of biomolecules onto PPNs. (a) fluorescence intensities of PPN-NB, PPN-Rho1, PPN-DOX, and PPN-Cur. (b) High-resolution C1s XPS spectra of all samples, including the unconjugated PPN. All data are presented as mean ± SD (n = 3). Statistical significance is denoted as follows: (****) $P < 0.0001$.

Comparable results were obtained with PPN-Rho1, where uptake by MDA-MB-231 cells was confirmed through the detection of fluorescence signals in the red channel (Figure **5**b). The cellular uptake studies demonstrate the adaptability of the PPN platform, allowing for the covalent conjugation of diverse fluorophores with distinct optical characteristics, a feature highly valuable for biomedical imaging applications. These results demonstrate that the PPN platform enables stable, linker-free conjugation of diverse fluorophores with distinct optical properties, supporting its adaptability for multimodal imaging in cancer diagnostics.

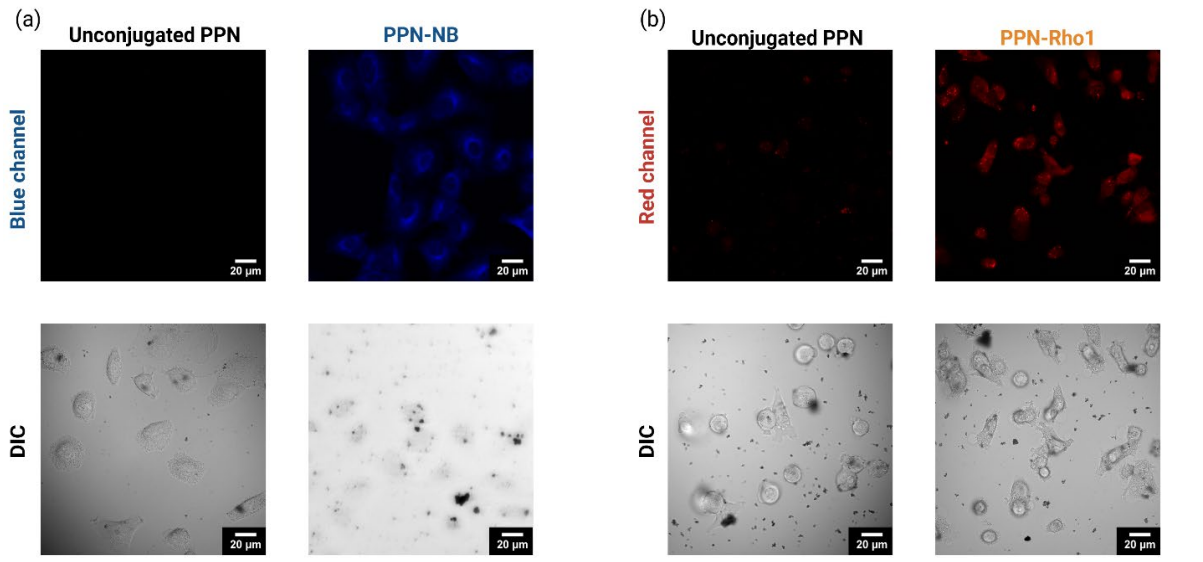

Figure 5: Successful cellular uptake is visualised using (a) PPN-NB in A549 lung cancer cells and (b) PPN-Rho1 in MDA-MB-231 breast cancer cells. In contrast, no fluorescence signals are observed in unconjugated PPNs which do not contain any fluorophores.

In addition to enabling diagnostic imaging, the PPN platform holds significant promise for targeted cancer therapy by facilitating site-specific delivery of therapeutic agents. Its stable, radical-rich surface

allows covalent conjugation of diverse drugs without the need for chemical linkers, offering a streamlined route to multifunctional nanocarriers.

To demonstrate this therapeutic potential, we conjugated two representative anticancer agents (DOX and Cur) onto PPNs, forming PPN-DOX and PPN-Cur, respectively (Figure **3**b). The nanocarriers were incubated with MDA-MB-231 triple-negative breast cancer cells over 72 hours. After the first 24 h, confocal microscopy imaging of PPN-Cur (Figure **6**a) and PPN-DOX (Figure **6**b) display successful localisation and internalisation of the conjugated PPNs onto the MDA-MB-231 cancer cells. Furthermore, both PPN-Cur and PPN-DOX were found to localise predominantly around the nucleus and along the cell membrane of cancer cells, a distribution pattern considered advantageous for drug delivery applications. In contrast, the unconjugated PPNs do not show any fluorescence signals (Figure **6**c), clearly indicating the need to tag with fluorescent molecules like Cur and DOX to track cellular uptake.

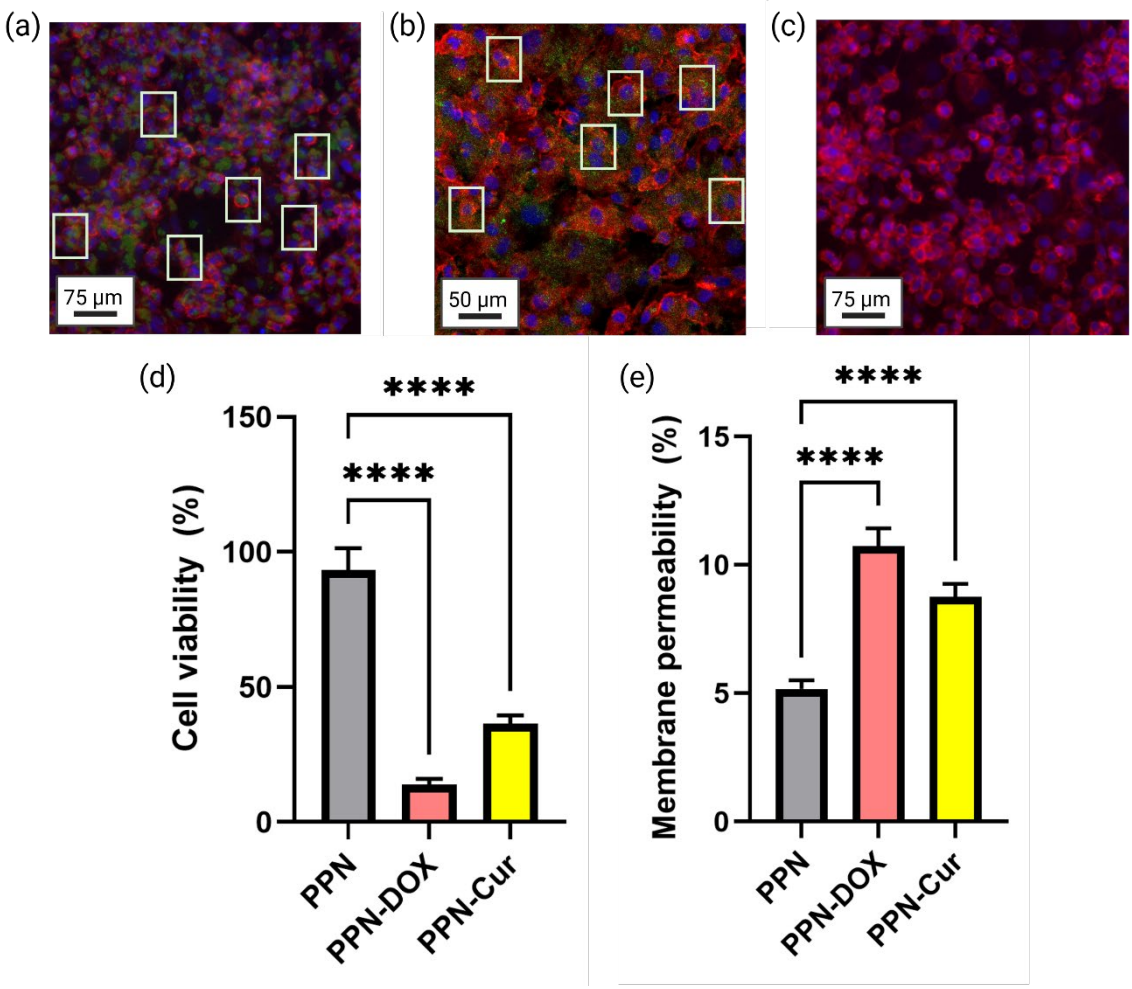

Figure 6: Payload-conjugated PPNs as drug delivery vehicles for cancer therapy. Fluorescence microscopy images of (a) PPN-Cur, (b) PPN-DOX, and (c) unconjugated PPN control samples dosed in MDA-MB-231 breast cancer cells for 24 h. (d) Alamar blue cytotoxicity assay and (e) LDH leakage assay. All data are presented as mean ± SD (n = 3). Statistical significance is denoted as follows: (****) $P < 0.0001$.

The successful internalisation of the payload-conjugated PPN translated to lower cell viabilities and higher membrane permeability of MDA-MB-231 cells as determined by Alamar Blue cytotoxicity assay and lactate dehydrogenase (LDH) leakage assay, respectively. Specifically, the cell viability and

proliferation of the breast cancer cells significantly decreased ($P < 0.0001$) from 93.91 ± 8.39% for the unconjugated PPN to 14.02 ± 2.22% and 35.85 ± 2.70% for PPN-DOX and PPN-Cur, respectively (Figure **6**d). The lower cell viability indicates cytotoxicity of both PPN-DOX and PPN-Cur towards MDA-MB-231 breast cancer cells. In addition, LDH leakage assay reveals an increase in membrane permeability upon introducing the cytotoxic payload-conjugated PPNs. LDH is a soluble enzyme found in the cytosol and is released into the cell culture medium once the cell membrane is ruptured. Membrane permeability, which has baseline levels at 5.17 ± 0.33% for the control PPN, spiked to 10.75 ± 0.68% for PPN-DOX, and to 8.76 ± 0.51% for PPN-Cur (Figure **6**e). These LDH leakage assay results corroborate with the cell internalisation and cytotoxicity studies, highlighting the potential of PPNs as viable nanoplatforms for drug delivery applications.

These findings establish the therapeutic potential of PPNs as an integrated nanoplatform capable of targeted delivery and cellular disruption, supporting their application in cancer nanomedicine. Beyond cancer therapy, these PPNs can be functionalised with other biomolecules for treating other diseases, sensitive biosensing, and cellular imaging applications.

Conclusion

This work demonstrates the promise of PPNs as multifunctional nanoplatforms that unite diagnostic imaging and therapeutic delivery in a single system. Through a one-step, chemical-free plasma process, diverse biomolecules were covalently conjugated onto PPN surfaces without the need for toxic solvents, linkers, or complex multi-step chemistry. Fluorophore-functionalised PPNs enabled real-time tracking of cellular uptake, while drug-conjugated PPNs achieved profound cytotoxic effects against triple-negative breast cancer cells, validating their therapeutic efficacy.

The sustainable and scalable plasma-based approach addresses long-standing barriers in nanomedicine by providing a green, modular, and clinically translatable strategy for cancer treatment. By integrating diagnosis and therapy into one adaptable carrier, PPNs represent not only a scientific advance but also a prototype with humanity at its core: a technology designed to transform cancer care while reducing environmental and manufacturing burdens.

Acknowledgements

Behnam Akhavan acknowledges the support of the Australian Research Council (ARC) through the DECRA program (DE210100662). The authors acknowledge the Sydney Nano Institute and the Hunter Medical Research Institute through the Precision Medicine Research Program. Elmer S. Austria Jr. acknowledges the support of the Faculty of Engineering Research Scholarship and the Career Advancement Award (PR4423/PR4424) from the University of Sydney. The authors would like to thank Dr. Ken Aldren S. Usman (Deakin University) and Prof. Joselito M. Razal (Deakin University) for access to the microscopy hub, and Prof. Elizabeth J. New (the University of Sydney) for generously providing the Rho1 fluorophore and access to confocal microscopy facilities. Austria and Akhavan also extend their sincere gratitude to Prof. Marcela M. M. Bilek (the University of Sydney) for her invaluable

guidance and mentorship. The authors gratefully acknowledge the facilities, technical, and scientific support provided by Sydney Microscopy and Microanalysis, the University of Sydney node of Microscopy Australia, and by Sydney Analytical, a core research facility at the University of Sydney.

References

Mattiuzzi, Camilla, and Giuseppe Lippi. "Current Cancer Epidemiology." *Journal of Epidemiology and Global Health* 9 (2019): 217–22. https://doi.org/10.2991/jegh.k.191008.001

Wang, Zihan, Qinzhou Ye, Sheng Yu, and Behnam Akhavan. "Poly Ethylene Glycol (Peg)-Based Hydrogels for Drug Delivery in Cancer Therapy: A Comprehensive Review." *Advanced Healthcare Materials* 12, no. 18 (2023): e2300105. https://doi.org/10.1002/adhm.202300105

Choudhurya, Hira, Manisha Pandey, Tan Hui Yin, Taasjir Kaur, Gan Wei Jia, S. Q. Lawrence Tan, How Weijie, et al. "Rising Horizon in Circumventing Multidrug Resistance in Chemotherapy with Nanotechnology." *Materials Science and Engineering: C* 101 (2019): 596–613. https://doi.org/10.1016/j.msec.2019.04.005

Su, Boyu, Shangkuo Li, Shuo Geng, Davide Brambilla, Rong Sun, Tao Sun, and Chen Jiang. "Therapeutic Regulation of Epigenetics in Cancer Treatment through Drug Delivery Systems." *Nano Today* 56 (2024): 102251. https://doi.org/10.1016/j.nantod.2024.102251

Dutta, Bijaideep, K. C. Barick, and P. A. Hassan. "Recent Advances in Active Targeting of Nanomaterials for Anticancer Drug Delivery." *Advances in Colloid and Interface Science* 296 (2021): 102509. https://doi.org/10.1016/j.cis.2021.102509

Mitchell, Michael J., Margaret M. Billingsley, Rebecca M. Haley, Marissa E. Wechsler, Nicholas A. Peppas, and Robert Langer. "Engineering Precision Nanoparticles for Drug Delivery." *Nature Reviews Drug Discovery* 20 (Feb 2021): 101–24. https://doi.org/10.1038/s41573-020-0090-8

Castro, Karine Cappuccio de, Josiel Martins Costa, and Maria Gabriela Nogueira Campos. "Drug-loaded Polymeric Nanoparticles: A Review." *International Journal of Polymeric Materials and Polymeric Biomaterials* 71, no. 1 (Aug 2020): 1–13. https://doi.org/10.1080/00914037.2020.1798436

Austria, Elmer S., Jr., and Behnam Akhavan. "Polymeric Nanoparticle Synthesis for Biomedical Applications: Advancing from Wet Chemistry Methods to Dry Plasma Technologies." *Nanoscale* 17, no. 21 (2025): 13020–56. https://doi.org/10.1039/D5NR00436E

Austria, Elmer, Jr., Marcela Bilek, Pegah Varamini, and Behnam Akhavan. "Breaking Biological Barriers: Engineering Polymeric Nanoparticles for Cancer Therapy." *Nano Today* 60 (2025): 102552. https://doi.org/10.1016/j.nantod.2024.102552

Santos, Miguel, Praveesuda L. Michael, Elysse C. Filipe, Alex H. P. Chan, Juichien Hung, Richard P. Tan, Bob S.L. Lee, et al. "Plasma Synthesis of Carbon-Based Nanocarriers for Linker-Free Immobilization of Bioactive Cargo." *ACS Applied Nano Materials* 1, no. 2 (Jan 2018): 580–94. https://doi.org/10.1021/acsanm.7b00086

Zhianmanesh, Masoud, Aaron Gilmour, Marcela M. M. Bilek, and Behnam Akhavan. "Plasma Surface Functionalization: A Comprehensive Review of Advances in the Quest for Bioinstructive Materials and Interfaces." *Applied Physics Reviews* 10, no. 2 (Apr 2023): 021301. https://doi.org/10.1063/5.0130829

Haidar, Laura Libnan, Yuheng Wang, Aaron D. Gilmour, Elmer Austria Jr., Badwi B. Boumelhem, Naveed Aziz Khan, Arifah Anwar Fadzil, Stuart T Fraser, Marcela M. M. Bilek, and Behnam Akhavan. "Direct Covalent Attachment of Fluorescent Molecules on Plasma Polymerized Nanoparticles: A Simplified Approach for Biomedical Applications." *Journal of Materials Chemistry. B* 13, no. 5 (2025): 1666–80. https://doi.org/10.1039/D4TB01515K

Akhavan, Behnam, Michiel Croes, Steven G. Wise, Chongpu Zhai, Juichien Hung, Callum Stewart, Mihail Ionescu, et al. "Radical-Functionalized Plasma Polymers: Stable Biomimetic Interfaces for Bone Implant Applications." *Applied Materials Today* 16 (2019): 456–73. https://doi.org/10.1016/j.apmt.2019.07.002

Haidar, Laura L., Mark Baldry, Stuart T. Fraser, Badwi Bob Boumelhem, Aaron D. Gilmour, Zongwen Liu, Zhong Zheng, Marcela M. M. Bilek, and Behnam Akhavan. "Surface-Active Plasma-Polymerized Nanoparticles for Multifunctional Diagnostic, Targeting, and Therapeutic Probes." *ACS Applied Nano Materials* 5, no. 12 (Aug 2022): 17576–91. https://doi.org/10.1021/acsanm.2c03213

Santos, Miguel, Bryce Reeves, Praveesuda Michael, Richard Tan, Steven G. Wise, and Marcela M. M. Bilek. "Substrate Geometry Modulates Self-Assembly and Collection of Plasma Polymerized Nanoparticles." *Communications Physics* 2, no. 52 (May 2019): 1–11. https://doi.org/10.1038/s42005-019-0153-5

Tan, Nian Kee, Hazel Chan, Zufu Lu, Hala Zreiqat, Girish Lakhwani, Pooria Lesani, and Elizabeth J. New. "Ultrasensitive Dual Fluorophore-conjugated Carbon Dots for Intracellular pH Sensing in 3d Tumor Models." *ACS Applied Materials & Interfaces* 16, no. 36 (Aug 2024): 47303–13. https://doi.org/10.1021/acsami.4c10836

Tacar, Oktay, Pornsak Sriamornsak, and Crispin R. Dass. "Doxorubicin: An Update on Anticancer Molecular Action, Toxicity and Novel Drug Delivery Systems." *Journal of Pharmacy and Pharmacology* 65, no. 2 (Feb 2013): 157–70. https://doi.org/10.1111/j.2042-7158.2012.01567.x

Shakori Poshteh, Shiva, Shohreh Alipour, and Pegah Varamini. "Harnessing Curcumin and Nanotechnology for Enhanced Treatment of Breast Cancer Bone Metastasis." *Discover Nano* 19, no. 177 (Nov 2024). https://doi.org/10.1186/s11671-024-04126-1